Powder Technology 224 (2012) 291–296

Contents lists available at SciVerse ScienceDirect

Powder Technology

journal homepage: www.elsevier.com/locate/powtec

The effects of the pressing step on the microstructure and aging of NdFeB bonded magnets

E.A. Périgo [a,*], M.F. de Campos [b], R.N. Faria [c], F.J.G. Landgraf [a,d]

[a] Institute for Technological Research (IPT), São Paulo, SP 05508-901, Brazil
[b] EEIMVR-Federal Fluminense University, Volta Redonda, RJ 27255-125, Brazil
[c] Nuclear and Energy Research Institute (IPEN), São Paulo, SP 05508-000, Brazil
[d] University of São Paulo, São Paulo, SP 05508-901, Brazil

ARTICLE INFO

Article history:
Received 16 January 2012
Received in revised form 13 February 2012
Accepted 8 March 2012
Available online 14 March 2012

Keywords:
NdFeB
Aging
Magnetic properties
Rietveld analysis

ABSTRACT

The effects of the compaction step on the (micro)structural features and aging behavior of polymer coated NdFeB-based bonded magnets is reported. Due to the fracture of the material during pressing, it is estimated an increase of at least 14% in the particles' area which is not coated. Such uncoated surfaces, when exposed to the environment, reduce the magnetic performance of the magnets aged/cured in air by 19% in the conditions evaluated in this investigation. Furthermore, XRD results interpreted by Rietveld analyses show a lattice parameter change in the tetragonal structure of the hard magnetic phase after pressing. Such change varies as a function of the height of the compacted part and it is ascribed to macro-elastic stress arising from the pressure distribution in the magnet. An aging/curing step during 24 h is able to relief such macro-elastic stress.

1. Introduction

The $RE_2TM_{14}B$ (RE=Nd or Pr and TM=Fe or Co) phase, also identified as Φ, possesses the highest maximum energy product (BH_{max}) among the available hard magnetic materials. Commercially, it can be found in magnets of mainly two classes: sintered or bonded. The former is produced by the usual powder metallurgy techniques [1,2] and the densification is obtained by a liquid phase sintering process promoted by the intergranular RE-rich phase. Concerning the latter, the parts are usually prepared from rapidly solidified alloys frequently coated with a compound responsible for the mechanical strength of the piece after pressing and aging (also known as curing if the period of time exposed to a given temperature is short) [3].

Analyzing the bonded magnets' production process in more details, it is possible to verify that the optimization of the starting material fabrication has already been reported [4] whereas the most favorable curing conditions are usually defined as a function of the compound used on the magnetic particles. On the other hand, a key processing parameter whose effects on the NdFeB magnets' microstructure which has not been investigated in details is the compaction step.

For the preparation of soft metallic magnetic parts by powder metallurgy, the compaction pressure (P) must be as high as possible to achieve a high magnetic permeability, magnetic polarization and low magnetic losses. Such property combination is possible due to the partial densification achieved by plastic deformation of the metal during pressing (typically ranging from 80% to 90% of the metal theoretical density). In bonded magnets P must also be high since remanence is proportional to density [5], but the Φ phase presents a plastic deformation degree much inferior compared to that of pure iron for instance, and a fracture should be expected. The sequence *pressing* → (*possible*) *plastic deformation* → (*possible*) *fracture* will play a significant role on the (micro)structural features and, consequently, on the aging magnitude of NdFeB-based particles which constitute bonded magnets. Furthermore, as the commercial applications of magnets are frequently exposed to temperatures above 120 °C, it is necessary to investigate the aging and accelerated trials are done in higher temperatures. A correlation processing – microstructure – aging comprises the outline of this work.

2. Experimental

The MQP-B powder was used as the stating material. Isotropic cylinders with height to diameter ratio of ~1 were prepared compacting the particles at 800 MPa at room temperature. No additional polymer, except the epoxy resin (density of about 600 kg m^{-3}) already existent on the surface of the particles, has been added before pressing. Next, pieces were aged at 200 °C during 1 h or 24 h under air or vacuum (pressure below 10^{-2} mbar). In order to separate the effects of the compaction pressure, the powders have also been exposed to the same aging conditions (only in air) to those of the magnets. It is worth mentioning that the aging step also acts as a

* Corresponding author. Tel.: +55 11 3767 4211; fax: +55 11 3767 4037.
E-mail address: eaperigo@ieee.org (E.A. Périgo).

0032-5910/$ – see front matter © 2012 Elsevier B.V. All rights reserved.
doi:10.1016/j.powtec.2012.03.010

curing procedure since it improves the mechanical strength of the parts.

The density of the pieces was obtained geometrically using the average of 3 cylinders. The magnetic properties of powders and magnets have been obtained with a vibrating sample magnetometer (VSM) and a hysteresisgraph, respectively, at room temperature. In both cases, the applied field to magnetize the samples was (2.0 ± 0.1) T and no demagnetization corrections have been employed. To perform the measurement of the not aged magnets (which shows low mechanical strength), the samples were surrounded by a tape. In order to obtain the remanence in Tesla, it has been considered $\rho_{NdFeB} = 7640\ kg\ m^{-3}$ [6].

The (micro)structural characterization has been performed by high-resolution SEM and X-ray diffraction (Co-Kα radiation—scanning rate of 0.5 degree min^{-1}) together with Rietveld analyses (TOPAS—academic software, v. 4.1), respectively. The XRD patterns have been obtained on orthogonal surfaces to the compaction direction in 2 distinct depths of the samples (top and bottom) to evaluate the presence of residual stresses along the parts.

In order to make easier the understanding of the results, they will be discussed based on characterization techniques.

3. Results and discussion

3.1. Magnetic and microstructural analyses

Fig. 1 shows the hysteresis curve of the powders before and after the aging procedure in air at 200 °C. The remanence (J_r) decreases with the aging time and the lowest value refers to the sample exposed to air during 24 h ($J_r = B_r = 0.83$ T). This value is about 6% inferior compared to that measured for the as-received material. Such variation is ascribed to the oxidation of the Φ phase because part of the coating is lost during the aging step. Such fact has been found because, after the aging procedure for 1 h, there is a mass loss of ~0.15%. Therefore, with the NdFeB-based particles' surfaces exposed to a rich oxygen environment, the volumetric fraction of the hard magnetic phase has been reduced causing the drop of J_r. Furthermore, this fact also explains the diminution of the magnetic polarization at $H > 1.5\ MA\ m^{-1}$. However, no oxide peaks were found; this fact might be related to XRD detection limit (minimum of ~5% in volume), which is similar to the reduction of the remanence (J_r and Φ volumetric fraction are proportional [7]). Regarding the intrinsic coercivity (H_c) of the powders, it has not been possible to observe any variation within the measurement error of the equipment (±1.5%). Therefore, it also indicates that this oxide thickness must be much smaller compared to the particle dimensions (~200 μm length and ~30 μm thickness). It is also worth mentioning that the initial magnetization curve provides an insight about the coercivity mechanism. According Stoner–Wohlfarth [8], when there is coherent rotation of single domain particles, the initial magnetization curve is exactly the average of the first and fourth quadrants of the hysteresis curve. This is the case for Fig. 1. The crystallite size estimated by Rietveld XRD is ~30 nm. This confirms that the grains are single domain. Thus, it is inferred that coherent rotation is the coercivity mechanism in these samples.

In order to characterize the microstructure of the powders prior to pressing, Fig. 2(A–B) depicts micrographs concerning the surface of NdFeB particles as-received and aged during 24 h in air, respectively. For low to medium magnifications (up to ~25,000×) the images are quite similar and even for higher magnifications it is not easy to identify relevant changes. It has been possible to observe in the former (as-received material) some roughness as well as regions which seem "individual" particles. On the other hand, the material aged for 24 h in air presents regions similar to the previous case, although these apparent "individual" particles have a smaller size (~50 nm) whose distribution is homogeneous.

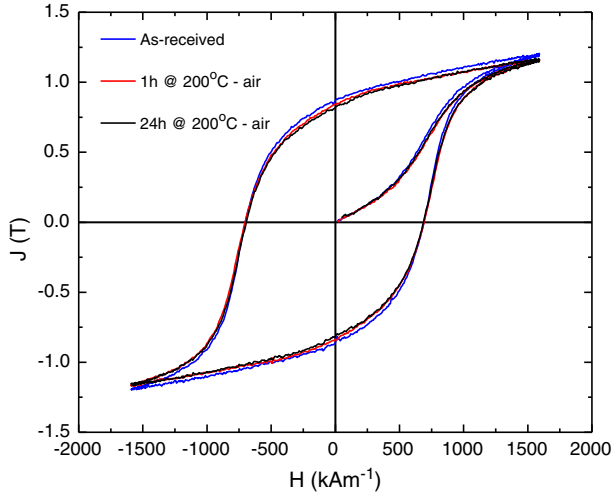

Fig. 1. $J \times H$ curves of the MQP-B powders before and after aging at 200 °C in air.

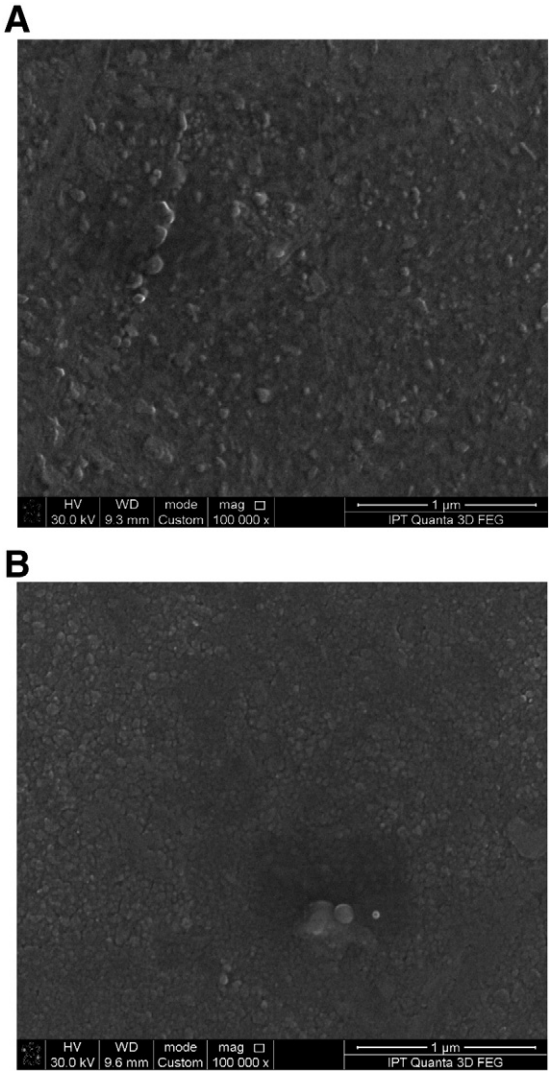

Fig. 2. HRSEM images of the MQP-B powders before (A) and after aging at 200 °C in air (B).

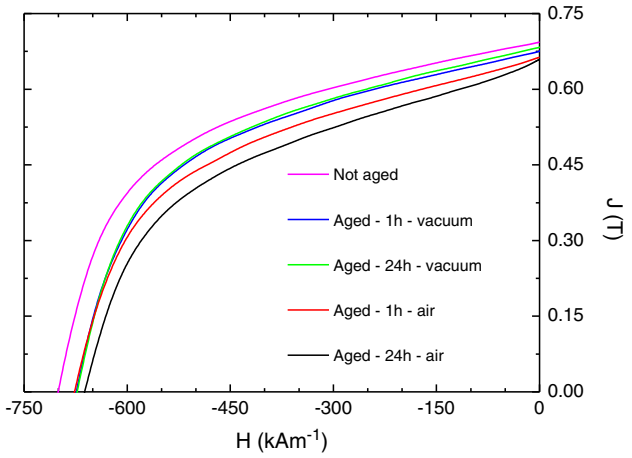

Fig. 3. $J \times H$ curves of the MQP-B magnets with and without aging.

A comparison of the second quadrant curves of the magnets is depicted in Fig. 3. The remanence of the not aged part agrees with the following expression

$$Jr_{magnet} = Jr_{powder} \cdot \frac{\rho_{magnet}}{\rho_{powder}}, \quad (1)$$

where Jr_{powder} is the remanence of the powder ((0.88 ± 0.02) T measured by VSM) and ρ_{magnet} and ρ_{powder} refer to the theoretical density of the powder and magnet ((5970 ± 50) kg m^{-3}), respectively. Eq. (1) assumes the proportionality of remanence with the saturation polarization, volumetric fraction and no crystallographic alignment of the hard magnetic phase during pressing [5,7]. All these parameters will be the same for both magnet and uncompressed powder, except the packing factor which is a function of density of both of them. Concerning the intrinsic coercivity, the value obtained for the compacted not-aged part is 2.5% lower to that verified for the powder. Although such discrepancy is almost twice the magnetic measurement experimental error, it is clear that the pressing has a reduced influence on H_c. Therefore, it is possible to consider that this result is in agreement with those previously reported, where H_c have not changed with compacting pressures up to 2.1 GPa [3].

Regarding aged parts, all magnetic properties are deleteriously affected after such heat treatment compared to powder and not-aged samples, independently on the atmosphere. Parts aged in air presented inferior magnetic performance compared to those aged under vacuum. The maximum energy product was the most affected magnetic property and has been reduced 19% for the piece aged during 24 h in air compared to not-aged pressed part, as listed in Table 1. This fact is attributed to the dependence of BH_{max} on the square of the remanence, i.e., a B_r reduction causes a doubled effect on the maximum energy product measured in the B–H curve. Furthermore, this sample also shows the lowest rectangularity of the $J \times H$ curve, determined by the squareness factor (SF) [9] also listed in Table 1, indicating that after aging such part presents an inferior stability to demagnetizing fields compared to the as-pressed magnet.

Table 1
Magnetic properties and squareness factor of the bonded magnets prepared in this work.

Sample/condition	J_r (T)	H_c (kA m^{-1})	BH_{max} (kJ m^{-3})	ΔBH_{max} (%)	SF (no unit)
	±1%	±1.5%	±2%		
Not aged	0.693	709.0	78.0	–	0.36
Aged – 1 h – vacuum	0.677	676.7	72.9	−6.5	0.33
Aged – 24 h – vacuum	0.683	682.0	73.9	−5.3	0.33
Aged – 1 h – air	0.663	686.0	67.4	−13.6	0.29
Aged – 24 h – air	0.659	672.2	63.3	−18.8	0.21

In order to explain this magnetic performance loss, a combination of the microstructural condition of NdFeB particles after pressing and aging must be analyzed. Fig. 4(A) shows a HRSEM image of the uncompressed powder. The particles usually present flat surfaces with no cracks and the dark spots refer to the coating of the material. On the other hand, Fig. 4(B–E) depicts the surface and the middle part of a not-aged compacted NdFeB magnet prepared with the same powder previously shown. In both regions of the piece the existence of cracks is evident, which exposes clean surfaces without coating. Besides, such cracks are partially or even completely through the particles, creating new particles with smaller size (but apparently not in nanometer scale) whose surfaces are clean (not oxidized and coated). Therefore, considering that typical NdFeB bonded magnets possess a minimum of 10% porosity (assuming that a compound of magnetic powder and organic binders can reach 6900 kg m^{-3} [3]) the gasses which constitute the aging atmosphere (which might include oxygen) will permeate through the sample causing a possible oxidation reaction with the clean surfaces (without coating) of the magnet. The magnetic performance of the pieces aged under vacuum is superior to those prepared in air because the partial pressure of oxygen has been reduced in the former. Moreover, the magnet aged during 24 h in air shows the worst magnetic properties because this has been the longest period of time that the compacted part, with surfaces without coating, has been exposed to an environment rich in oxygen. However, as previously informed, no oxide peaks have been found in any of the XRD patterns of the magnets.

In order to quantify how significant is the pressing influence on the microstructure of NdFeB-based bonded magnets, it is estimated the new exposed area (without coating) due to fracture of the material. To do so, it is assumed that an original particle (before pressing) is a rectangular bar with $30 \times 30 \times 200$ μm. After pressing, it is considered that each particle fractures in three parts across its thickness (as depicted in Fig. 4(B)). Therefore, four new and clean surfaces with 900 μm^2 each (3600 μm^2 total) would be created, which correspond to 14% of the original coated particle area. However, it is worth pointing out that such number might be underestimated because in the micrographs depicted in this work it is possible to observe that several particles also show more than 2 fractures.

Beyond the deleterious effect of the oxidation on the magnetic performance of NdFeB bonded magnets, it should also be pointed out that part of such magnetic loss must be attributed to the spin relaxation. This loss component tends to occur when the magnet is initially exposed to elevated temperatures for a period where oxidation might have not occurred [10]. Such effect has not been individually quantified because it has been assumed that its influence on the investigated powders and magnets are of minor importance compared to the oxidation effect.

3.2. XRD and Rietveld analyses

In order to analyze the existence of residual stresses in the NdFeB-based particles, Fig. 5 depicts a comparison of the XRD patterns of the powder, not-aged and aged compacted parts. Within the 2θ range shown, there is an increase of the intensity of peaks of the compacted material compared to that of the powder. This fact is ascribed to the higher density of the former. Furthermore, although a broadening of the diffraction peaks of the Φ phase is observed, the full width at half maximum (FWHM) is similar; this is an evidence of micro residual stress absence. A comparable XRD pattern has been obtained for the bottom part of the aged magnet, as also shown in Fig. 5. This last comparison indicates that the pressure has not been homogenously distributed along the magnet, since the peak intensity is slightly different. This should be expected because in the pressing

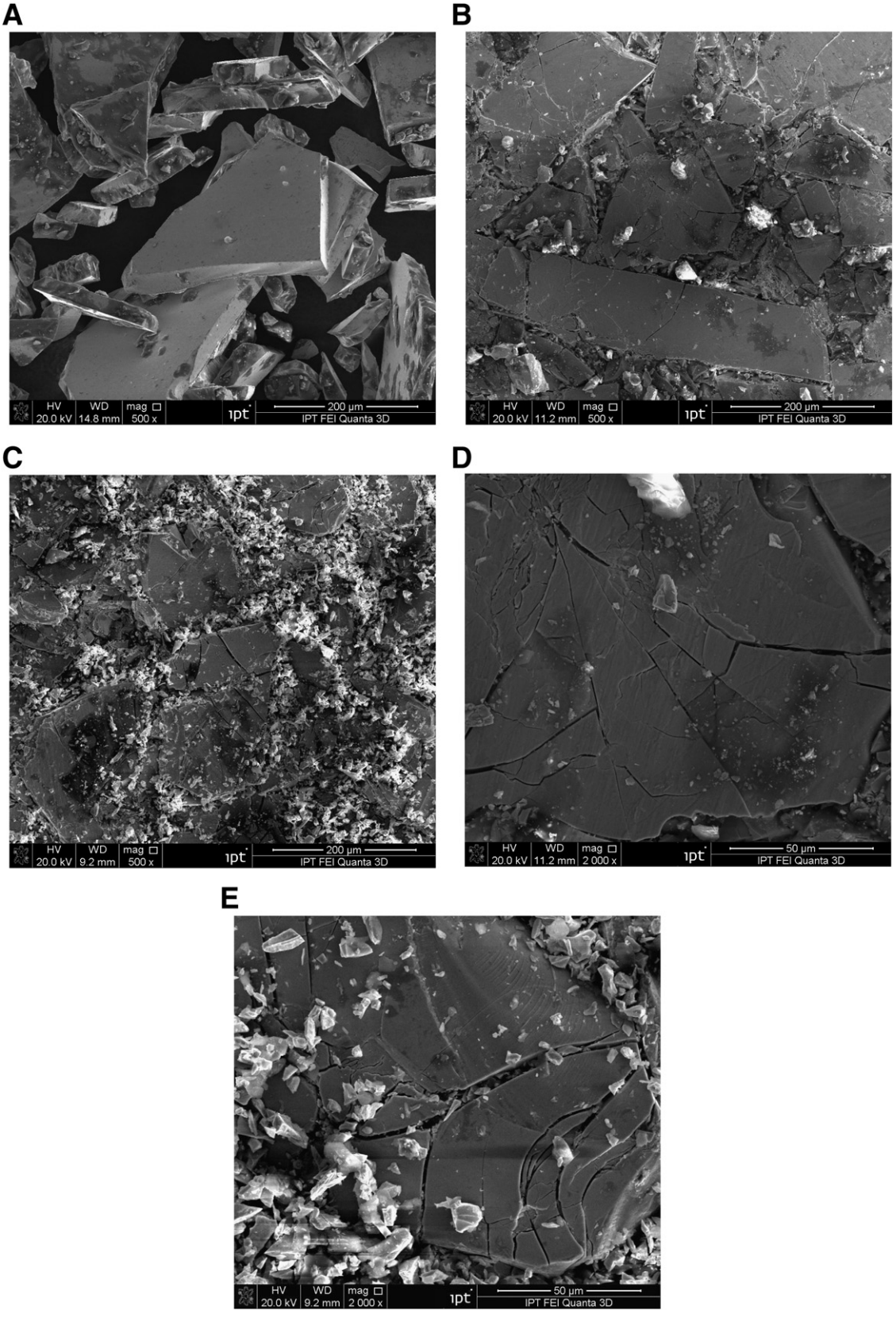

Fig. 4. HRSEM images of the NdFeB-based powder prior pressing (A), and after pressing on top part (B–D) and middle part (C–E).

system employed in this work (uniaxial), the force is applied on the top part of the sample. It is known that the pressure decreases exponentially with depth of the die cavity [11] and, therefore, the density usually presents a gradient which is a function of the height to diameter ratio as well as the friction of the particles among themselves and with the die wall.

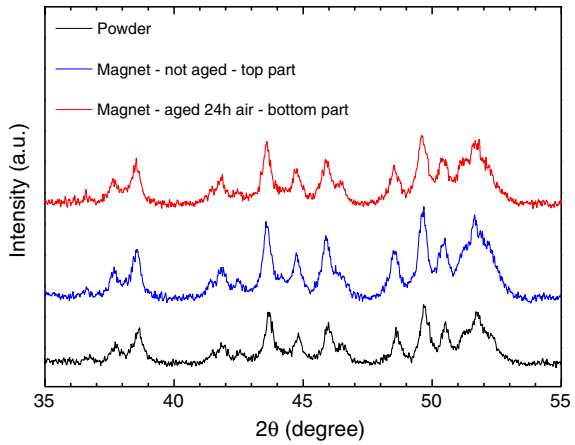

Fig. 5. Comparative XRD patterns of the powder, not aged and aged compacted at distinct positions.

Considering the existence of the density gradient, it should be expected that residual stresses, if they exist, would also present a gradient. Table 2 lists the lattice parameters, the macro-elastic residual stress, the volumetric fraction of phases in the powder and magnets (before and after aging) and the weighted profile R-factor (R_{wp}) of the simulations determined by Rietveld analysis. The *a* and *c* values found for the NdFeB-based powder are within ±0.5% compared to those previously reported by Herbst for the $Nd_2Fe_{14}B$ structure [12]. On the top part of the not-aged bonded magnet, lattice parameters are smaller than those of the powders and, at the bottom of the part, *a* and *c* values are intermediate between the powder and the top region. Such result is in agreement with the pressure distribution of an uniaxial compacting system.

The macro-elastic residual stress (σ) in each position of the compacted magnets, for several crystallographic planes, has been estimated using the expression:

$$\sigma = E \cdot \varepsilon \tag{2}$$

where *E* is the Young modulus and ε is the deformation obtained by using the lattice parameters of the Φ phase. A complete description of the employed methodology can be found in Ref. [13] and the elasticity modulus has been assumed as $E_{NdFeB} = 150$ GPa based on reported data [14,15]. To determine σ_{001} and σ_{100}, it has been used *a* and *c* values themselves; regarding σ_{111}, the interplanar distance has been found by using $\frac{1}{a^2} = \frac{h^2+k^2}{a^2} + \frac{l^2}{c^2}$, where *h*, *k* and *l* are the Miller indexes. The σ values are listed in Table 2 and for the not-aged sample it ranges between 120 and 200 MPa depending on the measurement position in the sample. The highest σ value (~200 MPa) is similar to the flexural stress reported for the NdFeB type sintered magnets [14]. After aging during 24 h in air, the lattice parameters return to the values previously found for the powder. Therefore, it seems that such "low temperature heat treatment" might also cause a stress relief in NdFeB-based particles after pressing. A typical Rietveld refinement of the XRD pattern of a bonded magnet is shown in Fig. 6. As can be verified, the simulated result is in well agreement with that obtained experimentally despite the $Nd_2Fe_{14}B$ is a low symmetry phase with a large number of diffraction peaks with low intensity. Furthermore, it is worth mentioning that there is no crystallographic texture in the samples. There is no peak exhibiting larger (or lower) intensity than that predicted for a random sample. In this kind of bonded magnet, texture can be introduced by means of magnetic field, which aligns the easy axis of the grains parallel to the applied field. However, magnetic fields were not applied during the processing.

Concerning the phase distribution in the magnetic material before and after pressing and aging, the Rietveld results are similar for all

Table 2
Lattice parameters, macroelastic stresses and volumetric fraction of the phases of NdFeB-based powder and magnets.

Sample/condition	*a* (nm)	*c* (nm)	σ[a] (MPa)	Φ (vol.%)	Fe (vol.%)	Nd_2O_3 (vol.%)	R_{wp} (%)
MQP-B powder	0.8805	1.2213	–	97	<3	<1	17.075
Magnet (not aged-top)	0.8792	1.2198	200	96	<3	<1	15.520
Magnet (not aged–bottom)	0.8798	1.2203	120	96	<3	<1	15.759
Magnet (aged – bottom – 24 h – air)	0.8805	1.2213	–	97	<3	<1	17.094

[a] Average of the values found for the planes (001), (100) and (111).

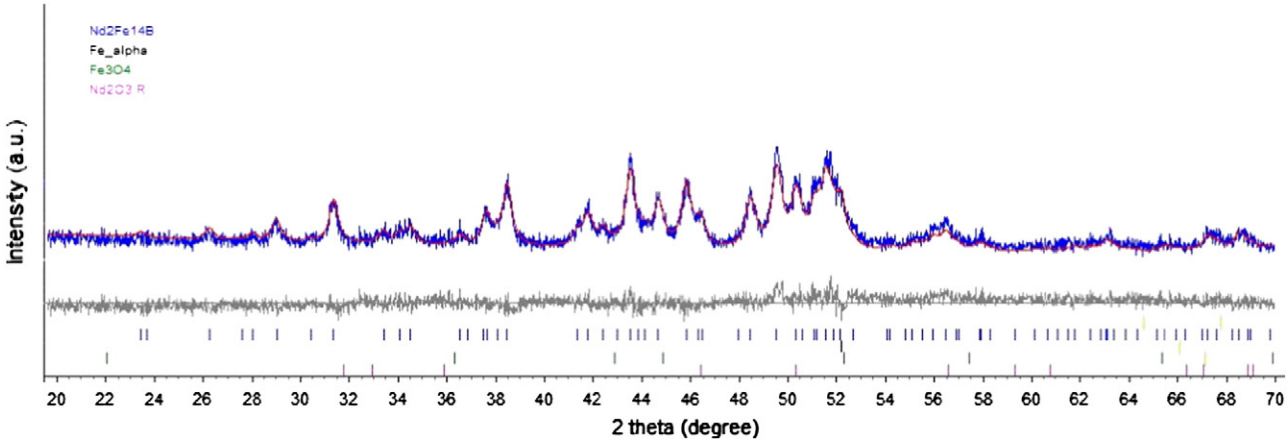

Fig. 6. Typical Rietveld analysis of the NdFeB-based compound. Blue line: experimental XRD pattern; Red line: simulated XRD pattern; Gray line: difference between experimental and simulated patterns.

samples, with the Φ phase as the major constituent and secondary phases (α-Fe and Nd_2O_3) with much smaller amounts (<3 and <1%, respectively). At last, the weighted profile R-factors (R_{wp}) might be considered acceptable taking into account the large number of peaks in the 2θ range analyzed. Furthermore, R_{wp} also depends on the employed software [16] and, for TOPAS, it might be higher than the R_{wp} obtained in other software.

4. Conclusions

Melt spun NdFeB-based particles used to prepare bonded magnets present a fragile fracture when compacted at 800 MPa. Due to porosity of the part, the existent oxygen in the environment permeates through the magnet and reacts with uncoated surfaces exposed due to the fractures arising from the pressing and cause a loss of the magnetic performance. It was estimated that the uncoated area exposed due to the formation of new particles is 14%; however, this number might be underestimated because several particles also show more than 2 fractures.

The most affected magnetic property was the maximum energy product, which reduced 19% after aging during 24 h in air compared to a non-aged part. Such effect is reduced when the aging is performed under vacuum, since the partial oxygen pressure has been reduced. Concerning remanence and intrinsic coercivity, they are also affected but at lower magnitude compared to that of BH_{max}. The coherent rotation is the coercivity mechanism in these samples.

The compaction step at 800 MPa reduces the lattice parameter of the $Nd_2Fe_{14}B$-based compound tetragonal structure, indicating the presence of a residual macro-elastic stress of compressive character of about 200 MPa. This value is similar to the flexural stress of NdFeB type sintered magnets. After aging, the lattice parameters of the hard magnetic phase are the same of the uncompressed powder. Therefore, it seems that aging step also has the ability to cause the stress relief of compacted NdFeB-based parts.

Acknowledgments

The authors are in debt to A.P. Braga and J. A. Provin for the HRSEM images, R. Martin for supporting the magnetic measurements and Dr. B. Grieb for providing the magnetic powder. E. A. Périgo thanks FAPESP for the partial financial support (proc. 2010/08018-8) and IPT for its facilities. M. F. de Campos thanks FAPERJ and CNPq.

References

[1] S. Guo, Q.Y. Zhou, R.J. Chen, D. Lee, A.R. Yan, Microstructure and magnetic properties of sintered Nd–Fe–B magnets with high hydrogen content, Journal of Applied Physics 109 (2011) 07A734.
[2] F. Xu, L. Zhang, X. Dong, Q. Liu, M. Komuro, Effect of DyF_3 additions on the coercivity and grain boundary structure in sintered Nd–Fe–B magnets, Scripta Materialia 64 (2011) 1137–1140.
[3] J. Herchenroeder, et al., High performance bonded neo magnets using high density compaction, Journal of Applied Physics 109 (2011) 07A743.
[4] C. Wang, M. Yan, Surface quality, microstructure and magnetic properties of Nd2(Fe, Zr, Co)14B/α-Fe alloys prepared by different melt-spinning equipments, Materials Science and Engineering B 164 (2) (2009) 71–75.
[5] R.N. Faria, The influence of zirconium addition and process parameters on the magnetic properties of Pr–Fe–B sintered magnets, Journal of Magnetism and Magnetic Materials 238 (1) (2002) 56–64.
[6] Magnequench catalog (2010), available on http://www.mqitechnology.com/isotropic.jsp, accessed Nov/10/2011.
[7] L.Q. Yu, J. Zhang, S.Q. Hu, Z.D. Han, M. Yan, Production for high thermal stability NdFeB magnets, Journal of Magnetism and Magnetic Materials 320 (2008) 1427–1430.
[8] E.C. Stoner, E.P. Wohlfarth, A mechanism of magnetic hysteresis in heterogeneous alloys, IEEE Transactions on Magnetics 27 (1991) 3475–3518.
[9] E.A. Périgo, H. Takiishi, C.C. Motta, R.N. Faria, On the squareness factor behavior of RE–FeB (RE═Nd or Pr) magnets above room temperature, IEEE Transactions on Magnetics 45 (10) (2009) 4431–4434.
[10] D.N. Brown, Z. Chen, P. Guschl, P. Campbell, Developments with melt spun RE–Fe–B powder for bonded magnets, Journal of Magnetism and Magnetic Materials 303 (2006) e371–e374.
[11] R.M. German, Powder Metallurgy Science, MPIF, New Jersey, 1984.
[12] J.F. Herbst, $R_2Fe_{14}B$ materials: intrinsic properties and technological aspects, Review of Modern Physics 63 (4) (1991) 819–898.
[13] E.A. Périgo, et al., Effects of the compaction pressure on the magnetic properties of a sintered Fe-based alloy, IEEE Transactions on Magnetics (2012), doi:10.1109/TMAG.2011.2173757.
[14] Y.M. Rabinovich, et al., Physical and mechanical properties of sintered Nd–Fe–B type permanent magnets, Intermetallics 4 (1996) 641–645.
[15] P. Vedrine, et al., Mechanical characteristics of NdFeB magnets at low temperature, Cryogenics 31 (1991) 51–53.
[16] B.H. Toby, R factors in Rietveld analysis: how good is good enough? Powder Diffraction 21 (1) (2006) 67–70.